Short communication

Na[FSA]-[C₃C₁pyrr][FSA] ionic liquids as electrolytes for sodium secondary batteries: Effects of Na ion concentration and operation temperature

Changsheng Ding [a], Toshiyuki Nohira [a, *], Rika Hagiwara [a, *], Kazuhiko Matsumoto [a], Yu Okamoto [a], Atsushi Fukunaga [b], Shoichiro Sakai [b], Koji Nitta [b], Shinji Inazawa [b]

[a] Graduate School of Energy Science, Kyoto University, Sakyo-ku, Kyoto 606-8501, Japan
[b] Electronics & Materials R&D Laboratories, Sumitomo Electric Industries, Ltd., Konohana-ku, Osaka 554-0024, Japan

HIGHLIGHTS

- Na[FSA]-[C₃C₁pyrr][FSA] ionic liquids were studied for sodium secondary batteries.
- The effects of Na ion concentration and operation temperature were evaluated.
- The Na ion concentration strongly affects the rate capability.
- The best rate capability at 363 K is obtained at 40 mol% Na[FSA].
- At temperatures below 273 K, the optimum Na ion concentration is 25 mol% Na[FSA].

ARTICLE INFO

ABSTRACT

As electrolytes for sodium secondary batteries operating over a wide temperature range, Na[FSA]-[C₃C₁pyrr][FSA] (FSA = bis(fluorosulfonyl)amide, C₃C₁pyrr = N-methyl-N-propylpyrrolidinium) ionic liquids have been investigated. The effects of Na ion concentration (0–60 mol% Na[FSA]) and operation temperature (253–363 K) on the viscosity and ionic conductivity and charge–discharge performance of Na/Na[FSA]-[C₃C₁pyrr][FSA]/NaCrO₂ cells are studied. Results show that Na ion concentration strongly affects the rate capability of the cells, and that the best rate capability at 363 K is obtained at 40 mol% Na[FSA]. The operation temperature also significantly influences the charge–discharge performance, especially at low temperatures. At operation temperatures below 273 K, 25 mol% Na[FSA] is found to be the optimum Na ion concentration. There exist different optimum ranges of Na ion concentration depending on the operation temperatures.

© 2014 Elsevier B.V. All rights reserved.

1. Introduction

As large-scale energy storage devices, sodium secondary batteries have been attracting much attention because of the low cost and abundant resources of sodium [1–6]. Na/S [7,8] and Na/NiCl₂ [9,10] batteries have been researched and partially commercialized. However, these commercialized sodium secondary batteries can only be operated at high temperatures (523–573 K) because solid β″-alumina electrolyte exhibits high ionic conductivity only at high temperatures. The high operation temperatures also result in an increase in the size, weight, and cost of the batteries. In the last few years, room temperature sodium secondary batteries have been intensively researched [1,2,11–16]. However, the reported room temperature sodium secondary batteries usually employ organic electrolytes such as NaClO₄/propylene carbonate (PC), which are disadvantageous for the construction of large-scale safe batteries, owing to their volatility and flammability. Moreover, the operation temperatures for such sodium secondary batteries are limited to a narrow temperature range around room temperature.

For application in electric vehicles (EVs) and hybrid electric vehicles (HEVs), secondary batteries are required to have high energy density, high safety, and a wide operation temperature range. Concerning the safety and operation temperature range, the

* Corresponding authors. Tel.: +81 75 753 5822; fax: +81 75 753 5906.
E-mail addresses: nohira@energy.kyoto-u.ac.jp (T. Nohira), hagiwara@energy.kyoto-u.ac.jp (R. Hagiwara).

technological bottleneck limiting the maxima lies in the electrolyte itself. Conventional organic electrolytes intrinsically do not meet the requirements of safety and wide operation temperature range. Thus, the key is to develop a new electrolyte that can be operated safely in a wide temperature range.

Ionic liquids, which consist entirely of cations and anions, generally provide negligibly low volatility, nonflammability, and high thermal and electrochemical stability [17—19]. Consequently, they have been studied and used as safe electrolytes in many electrochemical fields. For example, the ionic liquids Na[TFSA]-Cs[TFSA] (TFSA = bis(trifluoromethylsulfonyl)amide) [20] and Na[FSA]-K[FSA] (FSA = bis(fluorosulfonyl)amide) [21] have been investigated as electrolytes for sodium secondary batteries operating at intermediate temperatures. Na/Na[TFSA]-Cs[TFSA]/NaCrO$_2$ [20] and Na/Na[FSA]-K[FSA]/NaCrO$_2$ cells [21] exhibited a stable charge—discharge behavior at 423 and 353 K, respectively. However, these sodium secondary batteries can be operated only at intermediate temperatures because the melting points of these ionic liquids are higher than room temperature.

In view of this background, we focused on the ionic liquid [C$_3$C$_1$pyrr][FSA] (C$_3$C$_1$pyrr = *N*-methyl-*N*-propylpyrrolidinium), which has been reported to possess a low melting point (264 K), high conductivity (6.4 mS cm^{-1} at 298 K), and high thermal stability (up to 398 K) [22]. We have revealed that the ionic liquid Na[FSA]-[C$_3$C$_1$pyrr][FSA] has high ionic conductivity and a wide electrochemical window, and thus, it is a promising electrolyte for sodium secondary batteries [23,24]. A Na/Na[FSA]-[C$_3$C$_1$pyrr][FSA]/NaCrO$_2$ cell with 20 mol% Na[FSA] was successfully operated at 298 and 363 K [23]. However, other concentrations of Na[FSA] and other operation temperatures have not been investigated. When the concentration of Na[FSA] is optimized, higher performance and wider operation temperature range are expected for the cell. Here, we report the effects of Na ion concentration (0—60 mol% Na[FSA]) and operation temperature (253—363 K) on the viscosity, ionic conductivity and charge—discharge performance of Na/Na[FSA]-[C$_3$C$_1$pyrr][FSA]/NaCrO$_2$ cells. We also discuss the optimum Na ion concentration depending on the operation temperature.

2. Experimental

Na[FSA] (>99.0%, Mitsubishi Materials Electronic Chemicals, Japan) and [C$_3$C$_1$pyrr][FSA] (>99.9%, Kanto Chemical Co., Japan) were purchased and dried under vacuum at 333 K for 24 h. Na[FSA]-[C$_3$C$_1$pyrr][FSA] ionic liquids with Na ion concentration of 10—60 mol% Na[FSA] were prepared by mixing Na[FSA] and [C$_3$C$_1$pyrr][FSA] in an argon-filled glove box. The viscosities at different temperatures of the Na[FSA]-[C$_3$C$_1$pyrr][FSA] ionic liquids were measured by a viscometer (Brookfield Engineering Laboratories, DV-II + PRO). The ionic conductivities at different temperatures of the Na[FSA]-[C$_3$C$_1$pyrr][FSA] ionic liquids were measured by an AC impedance method using a calibrated cell with two platinum plate electrodes. The cell constant was determined using standard KCl aqueous solution.

NaCrO$_2$ powder was synthesized by mixing Na$_2$CO$_3$ and Cr$_2$O$_3$ and baking the mixture at 1123 K for 5 h under Ar flow. A composite positive electrode film consisting of 80 mass% NaCrO$_2$, 15 mass% acetylene black, and 5 mass% polytetrafluoroethylene was prepared and pressed onto an aluminum mesh current collector. A glass fiber filter (Whatman, GF-A, 260 mm) was used as a separator and metallic sodium was used as the negative electrode. Positive electrodes and separators were vacuum-impregnated with the Na[FSA]-[C$_3$C$_1$pyrr][FSA] ionic liquids at 333 K before assembling the cells. R2032-type coin cells, denoted as Na/Na[FSA]-[C$_3$C$_1$pyrr][FSA]/NaCrO$_2$ cells, were assembled in the argon-filled glove box. Charge—discharge tests for the Na/Na[FSA]-[C$_3$C$_1$pyrr][FSA]/

NaCrO$_2$ cells with different Na ion concentration were conducted at constant current rates of 20—2000 mA g^{-1} in the voltage range of 2.5—3.5 V at 253—363 K.

3. Results and discussion

Viscosities of the Na[FSA]-[C$_3$C$_1$pyrr][FSA] ionic liquids with 0—60 mol% Na[FSA] at different temperatures are shown in Fig. 1a. The viscosity increases with increase in the Na ion concentration. Similar phenomenon has also been observed for the Na[FSA]-[C$_2$C$_1$im][FSA] (C$_2$C$_1$im: 1-ethyl-3-methylimidazolium) [25], Na[TFSA]-[C$_2$C$_1$im][TFSA] [26], and Na[TFSA]-[C$_4$C$_1$pyrr][TFSA] (C$_4$C$_1$pyrr: *N*-butyl-*N*-methylpyrrolidinium) [27] ionic liquid systems. The increase in viscosity is probably attributed to the strong interaction between Na$^+$ cation and FSA$^-$ anion, forming ion pairs/clusters [26,28]. Nevertheless, the viscosity of the Na[FSA]-[C$_3$C$_1$pyrr][FSA] ionic liquid decreases as the temperature rises. In the case of 40 mol% Na[FSA], the viscosity significantly decreases from 1180 mPa s at 278 K to 30.4 mPa s at 353 K.

Fig. 1b shows the dependence of ionic conductivity on the Na[FSA] concentration at different temperatures. As expected from the results of viscosity, the ionic conductivity decreases when the Na ion concentration increases. However, the ionic conductivity can be largely improved by the elevation of temperature. For instance, the ionic conductivity of an IL containing 40 mol% Na[FSA] is as low
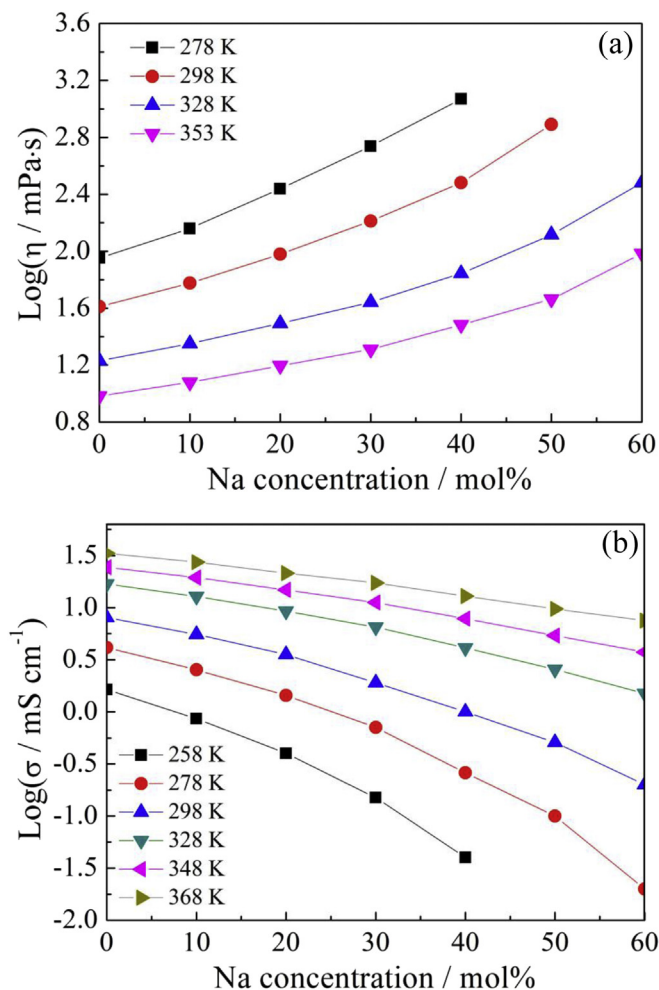

Fig. 1. Dependences of (a) viscosity and (b) ionic conductivity on the Na[FSA] concentration of Na[FSA]-[C$_3$C$_1$pyrr][FSA] ionic liquid at different temperatures.

as 0.04 mS cm^{-1} at 258 K. It increases, however, to 13 mS cm^{-1} at 368 K. For an IL containing 20 mol% Na[FSA], which corresponds to approximately 1 mol dm^{-3} Na[FSA], the ionic conductivity is 3.6 mS cm^{-1} at 298 K. This value is slightly lower than that of conventional NaClO$_4$/PC electrolyte at 1 mol dm^{-3} at 298 K (5−6 mS cm^{-1}) [29]. However, the conductivity of 20 mol% Na[FSA] system can be elevated to as high as 21 mS cm^{-1} at 368 K, at which the conventional organic electrolytes cannot be used.

Fig. 2a shows the discharge curves at current rates of 50−2000 mA (g-NaCrO$_2$)$^{-1}$ for a Na/Na[FSA]-[C$_3$C$_1$pyrr][FSA]/NaCrO$_2$ cell with 40 mol% Na[FSA] at 363 K. Here, the current rate for charge and discharge processes is the same. When the theoretical capacity of NaCrO$_2$ is defined as 125 mAh (g-NaCrO$_2$)$^{-1}$ ($0.5 \leq x \leq 1$ in Na$_x$CrO$_2$), 50 and 2000 mA (g-NaCrO$_2$)$^{-1}$ correspond to 0.4C and 16C in the C-rate, respectively. The discharge capacities and coulombic efficiency for different current rates are shown in Fig. 2b. The shape of the charge−discharge curves at 50 mA (g-NaCrO$_2$)$^{-1}$ is the same for those reported previously [30,31]. The composition-driven structural changes observed during the charge or desodiation process occur in the following sequence: rhombohedral O3, monoclinic O′3, and monoclinic P′3 structures [30,31]. The discharge capacity decreases gradually with increase in the charge−discharge rate. At 500 mA (g-NaCrO$_2$)$^{-1}$, the discharge capacity is 96 mAh (g-NaCrO$_2$)$^{-1}$ and about 90% of the capacity at 50 mA (g-NaCrO$_2$)$^{-1}$ is maintained. The discharge capacity decreases to 76 mAh (g-NaCrO$_2$)$^{-1}$ at a high rate of 2000 mA (g-

NaCrO$_2$)$^{-1}$, but it still corresponds to about 71% of the capacity at 50 mA (g-NaCrO$_2$)$^{-1}$. For all charge−discharge rates, except for the initial cycle, the coulombic efficiencies are higher than 99.5%. The cell also shows good cycle performance at each rate. These results demonstrate that the cell with 40 mol% Na[FSA] exhibits good rate capability and cyclability at 363 K.

We have reported the rate capability of the Na/Na[FSA]-[C$_3$C$_1$pyrr][FSA]/NaCrO$_2$ cell with 20 mol% Na[FSA] in a previous study [23]. It is expected that the cells would show different rate capabilities when the Na ion concentration in the ionic liquids is varied. Fig. 3 compares the rate capabilities of Na/Na[FSA]-[C$_3$C$_1$pyrr][FSA]/NaCrO$_2$ cells with 20, 30, 40, 50, and 60 mol% Na[FSA] at 363 K. At charge−discharge rates lower than 500 mA (g-NaCrO$_2$)$^{-1}$, the effect of Na ion concentration on the discharge capacity is very small. On the contrary, the Na ion concentration considerably affects the discharge capacity at charge−discharge rates higher than 500 mA (g-NaCrO$_2$)$^{-1}$. At the highest charge−discharge rate of 2000 mA (g-NaCrO$_2$)$^{-1}$, the discharge capacity increases with an increase in the Na ion concentration from 20 to 40 mol% Na[FSA]. When the Na ion concentration reaches 40 mol% Na[FSA], the cell shows the highest discharge capacity of 76 mAh (g-NaCrO$_2$)$^{-1}$. Then, the discharge capacity decreases with an increase in the Na ion concentration. This is because higher Na ion concentration leads to increased Na ion conductivity, but excess Na ion concentration also increases the viscosity of the ionic liquid, resulting in the decrease of Na ion conductivity. Thus, it is concluded that 40 mol% Na[FSA] is the optimum concentration for Na/Na[FSA]-[C$_3$C$_1$pyrr][FSA]/NaCrO$_2$ cell, which shows the best rate capability at 363 K.

To investigate the effect of operation temperature on the charge−discharge performance, Na/Na[FSA]-[C$_3$C$_1$pyrr][FSA]/NaCrO$_2$ cells with different Na ion concentrations (10, 15, 20, 25, and 30 mol% Na[FSA]) were tested from 363 K down to 253 K. As a typical result, Fig. 4a shows the charge−discharge curves of a cell with 25 mol% Na[FSA] at 253−363 K at current rate of 20 mA (g-NaCrO$_2$)$^{-1}$. The discrepancy of the plateau potentials between the charge and discharge curves is increased when the operation temperature is lowered. As a natural consequence, the discharge capacity is reduced when the temperature is decreased. It should be noted, however, that both the discrepancy of the plateau potentials and the decrease in capacity are scarcely observed at 298 K.
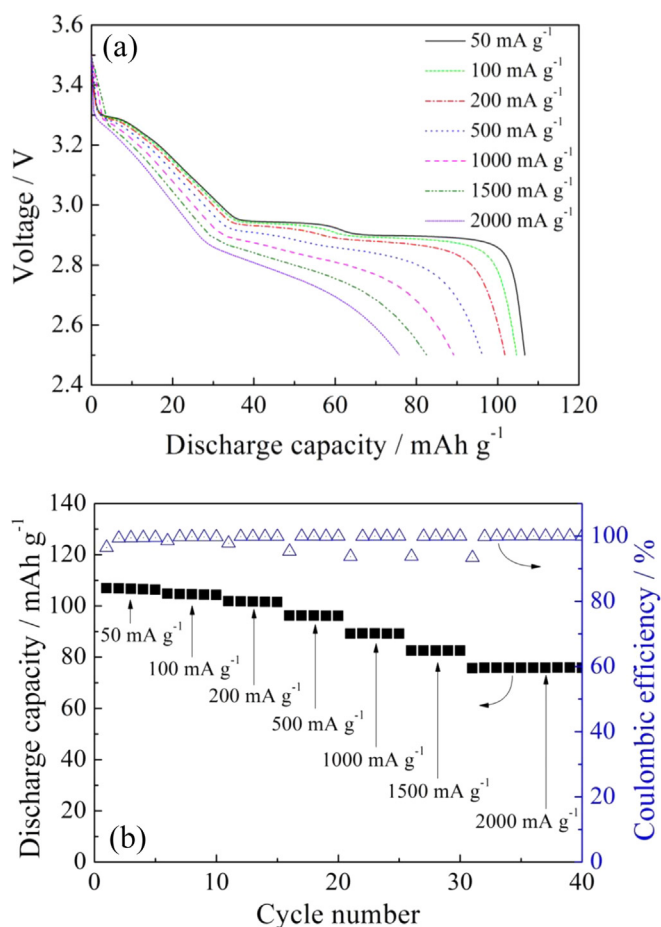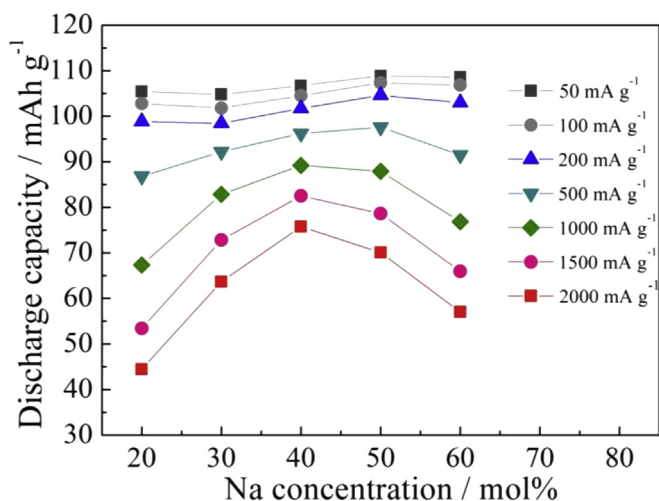

Fig. 2. Rate capability of a Na/Na[FSA]-[C$_3$C$_1$pyrr][FSA]/NaCrO$_2$ cell with 40 mol% Na [FSA] at 363 K: (a) discharge curves and (b) discharge capacities and coulombic efficiency. Charge−discharge rates: 50−2000 mA g^{-1}. Cut-off voltages: 2.5−3.5 V.

Fig. 3. Comparison of rate capability for Na/Na[FSA]-[C$_3$C$_1$pyrr][FSA]/NaCrO$_2$ cells with 20−60 mol% Na[FSA] at 363 K. Charge−discharge rates: 50−2000 mA g^{-1}. Cut-off voltages: 2.5−3.5 V.
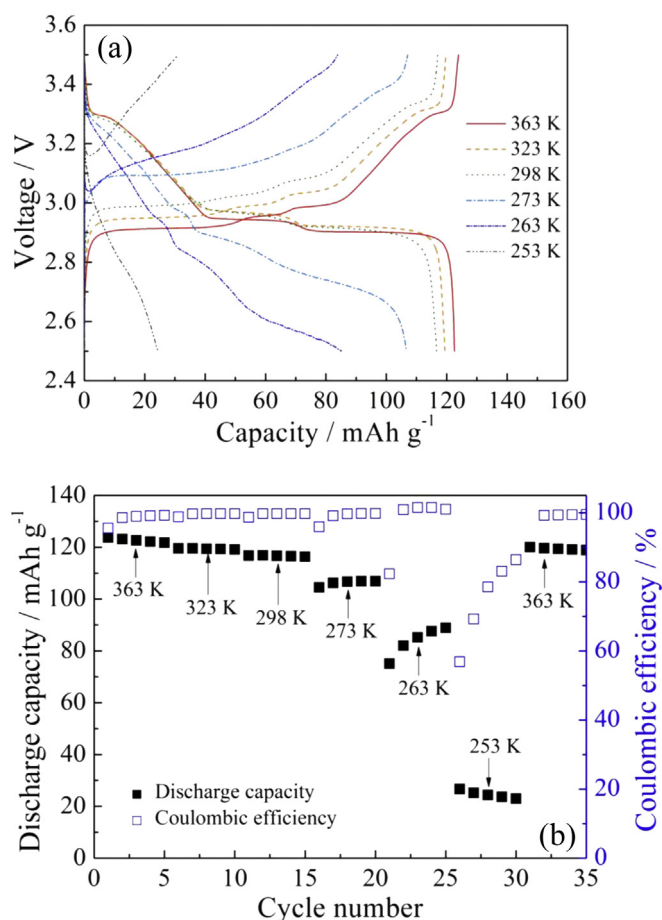
Fig. 4. Charge and discharge performance of a Na/Na[FSA]-[C$_3$C$_1$pyrr][FSA]/NaCrO$_2$ cell with 25 mol% Na[FSA] at 253−363 K: (a) charge−discharge curves and (b) discharge capacities and coulombic efficiency. Charge−discharge rate: 20 mA g^{-1}. Cut-off voltages: 2.5−3.5 V.

Fig. 4b shows the discharge capacities and coulombic efficiency of the cell with 25 mol% Na[FSA] at 253−363 K at a current rate of 20 mA (g-NaCrO$_2$)$^{-1}$. At 363 K, the discharge capacity is 123 mAh (g-NaCrO$_2$)$^{-1}$, which is very close to the theoretical capacity of 125 mAh (g-NaCrO$_2$)$^{-1}$. When the temperature is lowered from 363 K to 298 K, the discharge capacity decreases slightly to 117 mAh (g-NaCrO$_2$)$^{-1}$. For comparison, it was reported that a capacity of 104 mAh (g-NaCrO$_2$)$^{-1}$ was obtained at 298 K at a current rate of 5.0 mA (g-NaCrO$_2$)$^{-1}$, where 1 M NaClO$_4$/PC was used as an electrolyte [30]. Compared with the conventional organic electrolytes, the present ionic liquid electrolyte shows larger discharge capacity at 298−363 K, and is promising for the applications to EVs and HEVs. When the temperature becomes lower than 298 K, the discharge capacity further decreases. Nevertheless, a capacity of 106 mAh (g-NaCrO$_2$)$^{-1}$, corresponding to about 86% of the initial discharge capacity at 363 K, is still maintained at 273 K. At lower temperatures, 263 and 253 K, the cell delivers average discharge capacities of approximately 85 and 25 mAh (g-NaCrO$_2$)$^{-1}$, respectively. The lower capacity at low temperatures is attributed to the high internal resistance of cell, which arises from reduced ionic conductivity of electrolyte, lowered diffusivity of sodium ion in solid Na$_x$CrO$_2$, and increased charge-transfer resistance at electrode/electrolyte interfaces [32]. It should be noted, however, that the discharge capacity is almost fully recovered to the initial value when the temperature is raised to 363 K again. The coulombic efficiency is close to 100% except for the initial cycle at each

temperature and for all cycles at 253 K. As a result, the Na/Na[FSA]-[C$_3$C$_1$pyrr][FSA]/NaCrO$_2$ cell can be operable in a wide temperature range of 263−363 K. At a very low temperature, 253 K, the cell can discharge with a small capacity, which means that it is possible to start heating the battery by itself.

The Na/Na[FSA]-[C$_3$C$_1$pyrr][FSA]/NaCrO$_2$ cells with different Na ion concentrations show similar charge−discharge behaviors at low discharge rates of 20−50 mA (g-NaCrO$_2$)$^{-1}$ at 298−363 K. At lower temperatures of 253−273 K, however, the discharge capacities are different for cells with different Na ion concentrations. Fig. 5 compares the discharge capacities of the cells with 10, 15, 20, 25, and 30 mol% Na[FSA] at 253−363 K. As previously mentioned, the discharge capacities at 298−363 K are almost unaffected by the Na ion concentration. At temperatures below 273 K, the discharge capacity increases gradually with an increase in the Na ion concentration. At temperatures of 253, 263, and 273 K, the cell exhibits the highest discharge capacities at 25 mol% Na[FSA]. At 30 mol% Na [FSA], the discharge capacity decreases again, which is attributed to the opposing effect on ionic conduction caused by the increase of viscosity of the electrolyte. It is concluded that the cell with 25 mol % Na[FSA] exhibits the best electrochemical performance below room temperature.

4. Conclusion

We have investigated the use of Na[FSA]-[C$_3$C$_1$pyrr][FSA] ionic liquids as electrolytes for sodium secondary batteries operating over a wide temperature range of 253−363 K. The viscosity increases and the ionic conductivity decreases when the Na ion concentration in IL increases. By the elevation of temperature, however, ionic conductivities much higher than that of conventional organic electrolyte at room temperature can be achieved. Na ion concentration in the ionic liquids strongly affects the rate capability of a Na/Na[FSA]-[C$_3$C$_1$pyrr][FSA]/NaCrO$_2$ cell. The best rate capability at 363 K is obtained at 40 mol% Na[FSA]. The operation temperature also significantly influences the charge−discharge performance, especially at low temperatures, and the discharge capacity decreases gradually with decrease in the operation temperature. At operation temperatures below 273 K, 25 mol % Na[FSA] is found to be the optimum Na ion concentration. It is concluded that there exist different optimum ranges of Na ion concentration depending on the operation temperatures.
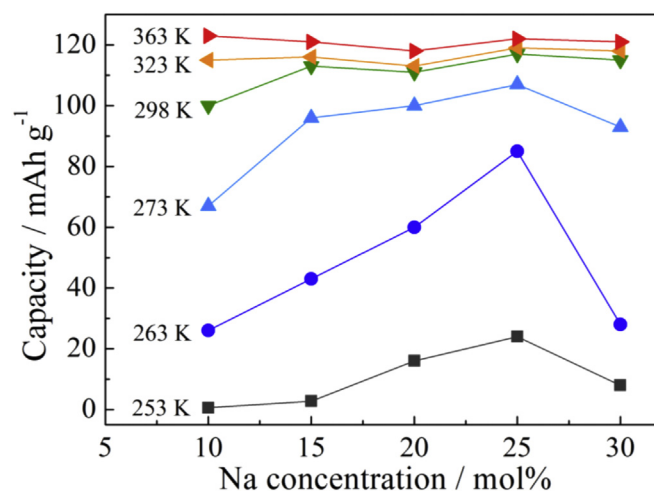

Fig. 5. Comparison of discharge capacities for Na/Na[FSA]-[C$_3$C$_1$pyrr][FSA]/NaCrO$_2$ cells with 10−30 mol% Na[FSA] at 253−363 K. Charge−discharge rate: 20 mA g^{-1}. Cut-off voltages: 2.5−3.5 V.

Acknowledgments

References

[1] S.W. Kim, D.H. Seo, X. Ma, G. Ceder, K. Kang, Adv. Energy Mater. 2 (2012) 710—721.
[2] R. Berthelot, D. Carlier, C. Delmas, Nat. Mater. 10 (2011) 76—80.
[3] N. Yabuuchi, M. Kajiyama, J. Iwatate, H. Nishikawa, S. Hitomi, R. Okuyama, R. Usui, Y. Yamada, S. Komaba, Nat. Mater. 11 (2012) 512—517.
[4] B.L. Ellis, L.F. Nazar, Curr. Opin. Solid State Mater. Sci. 16 (2012) 168—177.
[5] V. Palomares, P. Serras, I. Villaluenga, K.B. Hueso, J.C. Gonzalez, T. Rojo, Energy Environ. Sci. 5 (2012) 5884—5901.
[6] M.D. Slater, D. Kim, E. Lee, C.S. Johnson, Adv. Funct. Mater. 23 (2013) 947—958.
[7] J.L. Sudworth, J. Power Sources 11 (1984) 143—154.
[8] T. Oshima, M. Kajita, A. Okuno, Int. J. Appl. Ceram. Technol. 1 (2004) 269—276.
[9] J. Coetzer, J. Power Sources 18 (1986) 377—380.
[10] C.H. Dustmann, J. Power Sources 127 (2004) 85—92.
[11] Y. Yamada, T. Doi, I. Tanaka, S. Okada, J. Yamaki, J. Power Sources 196 (2011) 4837—4841.
[12] Y. Kawabe, N. Yabuuchi, M. Kajiyama, N. Fukuhara, T. Inamasu, R. Okuyama, I. Nakai, S. Komaba, Electrochem. Commun. 13 (2011) 1225—1228.
[13] S. Wenzel, T. Hara, J. Janek, P. Adelhelm, Energy Environ. Sci. 4 (2011) 3342—3345.
[14] D.H. Kim, S.H. Kang, M. Slater, S. Rood, J.T. Vaughey, N. Karan, M. Balasubramanian, C.S. Johnson, Adv. Energy Mater. 1 (2011) 333—336.
[15] H. Kim, R.A. Shakoor, C. Park, S.Y. Lim, J.S. Kim, Y.N. Jo, W. Cho, K. Miyasaka, R. Kahraman, Y. Jung, J.W. Choi, Adv. Funct. Mater. 23 (2013) 1147—1155.
[16] A. Ponrouch, E. Marchante, M. Courty, J.M. Tarascon, M.R. Palacin, Energy Environ. Sci. 5 (2012) 8572—8583.
[17] M. Galinski, A. Lewandowski, I. Stepniak, Electrochim. Acta 51 (2006) 5567—5580.
[18] M.J.A. Shiddiky, A.A.J. Torriero, Biosens. Bioelectron. 26 (2011) 1775—1787.
[19] M.A.P. Martins, C.P. Frizzo, D.N. Moreira, N. Zanatta, H.G. Bonacorso, Chem. Rev. 108 (2008) 2015—2050.
[20] T. Nohira, T. Ishibashi, R. Hagiwara, J. Power Sources 205 (2012) 506—509.
[21] A. Fukunaga, T. Nohira, Y. Kozawa, R. Hagiwara, S. Sakai, K. Nitta, S. Inazawa, J. Power Sources 209 (2012) 52—56.
[22] Q. Zhou, W.A. Henderson, G.B. Appetecchi, M. Montanino, S. Passerini, J. Phys. Chem. B 112 (2008) 13577—13580.
[23] C.S. Ding, T. Nohira, K. Kuroda, R. Hagiwara, A. Fukunaga, S. Sakai, K. Nitta, S. Inazawa, J. Power Sources 238 (2013) 296—300.
[24] A. Fukunaga, T. Nohira, R. Hagiwara, K. Numata, E. Itani, S. Sakai, K. Nitta, S. Inazawa, J. Power Sources 246 (2014) 387—391.
[25] K. Matsumoto, T. Hosokawa, T. Nohira, R. Hagiwara, A. Fukunaga, K. Numata, E. Itani, S. Sakai, K. Nitta, S. Inazawa, J. Power Sources 265 (2014) 36—39.
[26] D. Monti, E. Jonsson, M.R. Palacin, P. Johansson, J. Power Sources 245 (2014) 630—636.
[27] S.A.M. Noor, P.C. Howlett, D.R. MacFarlane, M. Forsyth, Electrochim. Acta 114 (2013) 766—771.
[28] A. Andriola, K. Singh, J. lewis, L. Yu, J. Phys. Chem. B 114 (2010) 11709—11714.
[29] K. Kuratani, N. Uemura, H. Senoh, H.T. Takeshita, T. Kiyobayashi, J. Power Sources 223 (2013) 175—182.
[30] S. Komaba, T. Nakayama, A. Ogata, T. Shimizu, C. Takei, S. Takada, A. Hokura, I. Nakai, ECS Trans. 16 (2009) 43—55.
[31] C.Y. Chen, K. Matsumoto, T. Nohira, R. Hagiwara, A. Fukunaga, S. Sakai, K. Nitta, S. Inazawa, J. Power Sources 237 (2013) 52—57.
[32] S.S. Zhang, K. Xu, T.R. Jow, J. Power Sources 115 (2003) 137—140.